Notch Signaling Is Antagonized by SAO-1, a Novel GYF-Domain Protein That Interacts with the E3 Ubiquitin Ligase SEL-10 in *Caenorhabditis elegans*

Valerie A. Hale, Evan L. Guiney, Lindsey Y. Goldberg, Josephine H. Haduong, Callie S. Kwartler, Katherine W. Scangos, and Caroline Goutte[1]
Department of Biology, Amherst College, Amherst, Massachusetts 01002

ABSTRACT Notch signaling pathways can be regulated through a variety of cellular mechanisms, and genetically compromised systems provide useful platforms from which to search for the responsible modulators. The *Caenorhabditis elegans* gene *aph-1* encodes a component of γ-secretase, which is essential for Notch signaling events throughout development. By looking for suppressors of the incompletely penetrant *aph-1(zu147)* mutation, we identify a new gene, *sao-1* (**s**uppressor of **a**ph-**o**ne), that negatively regulates *aph-1(zu147)* activity in the early embryo. The *sao-1* gene encodes a novel protein that contains a GYF protein–protein interaction domain and interacts specifically with SEL-10, an Fbw7 component of SCF E3 ubiquitin ligases. We demonstrate that the embryonic lethality of *aph-1(zu147)* mutants can be suppressed by removing *sao-1* activity or by mutations that disrupt the SAO-1–SEL-10 protein interaction. Decreased *sao-1* activity also influences Notch signaling events when they are compromised at different molecular steps of the pathway, such as at the level of the Notch receptor GLP-1 or the downstream transcription factor LAG-1. Combined analysis of the SAO-1–SEL-10 protein interaction and comparisons of *sao-1* and *sel-10* genetic interactions suggest a possible role for SAO-1 as an accessory protein that participates with SEL-10 in downregulation of Notch signaling. This work provides the first mutant analysis of a GYF-domain protein in either *C. elegans* or *Drosophila* and introduces a new type of Fbw7-interacting protein that acts in a subset of Fbw7 functions.

THE Notch signaling pathway plays a critical role in many cell-fate choices during animal development. Pathway activation begins with the interaction of a DSL (Delta/Serrate/Lag-2) ligand and a cell-surface Notch receptor. Upon ligand binding, the Notch receptor undergoes two sequential proteolytic cleavages: an ADAM-protease releases the extracellular domain and then γ-secretase releases the intracellular domain, which translocates to the nucleus. γ-Secretase is a complex of four integral membrane proteins (presenilin, APH-1, APH-2/Nicastrin, and PEN-2), which also cleaves a variety of other transmembrane protein substrates, including ERBB4 receptor tyrosine kinase, N-cadherin, and the amyloid-β precursor protein (APP) associated with Alzheimer's disease (Parks and Curtis 2007). Once in the nucleus, the Notch intracellular domain interacts with the conserved transcription factor CSL (CBF1/Suppressor of Hairless/LAG-1) to regulate transcription of target genes (reviewed in Kopan and Ilagan 2009).

There are two related Notch receptors in *C. elegans*, GLP-1 and LIN-12, which mediate a variety of cell interactions throughout development. In the early embryo, at least six distinct cell interactions are mediated by GLP-1 or LIN-12 and they serve to pattern the developmental fate of embryonic cells (reviewed in Priess 2005). The first two such signaling events occur at the 4-cell and 12-cell stages of embryogenesis and are mediated by maternally supplied signaling components including GLP-1. Removal of maternal GLP-1 or LAG-1, or any of the four γ-secretase components, prevents Notch signaling in these early stages of embryogenesis, resulting in misspecification of several blastomere fates and eventual arrest of the embryo (Priess 2005). At least some of the later embryonic signaling events can be mediated by either GLP-1 or LIN-12, such that a mutant phenotype is only apparent in these cell-fate choices if both receptors are absent (Lambie and Kimble 1991).

doi: 10.1534/genetics.111.136804
Manuscript received July 29, 2011; accepted for publication December 6, 2011
Supporting information is available online at http://www.genetics.org/content/suppl/2011/12/30/genetics.111.136804.DC1.
[1]Corresponding author: 2237 McGuire Life Sciences, Department of Biology, Amherst College, Amherst, MA 01002. E-mail: cegoutte@amherst.edu

During postembryonic development GLP-1 and LIN-12 have distinct roles. GLP-1 activation is required continuously to induce germ cell proliferation in the distal gonad, thus playing a critical role in regulating the balance between proliferation and meiosis (Kimble and Crittenden 2005). Loss of GLP-1 activity results in sterility due to germ line under proliferation, whereas hyperactive GLP-1 protein causes overproliferation of the germ line at the expense of germ cell differentiation (Berry *et al.* 1997; Pepper *et al.* 2003; Kimble and Crittenden 2005). LIN-12 is largely responsible for mediating cell interactions that dictate somatic cell fate choices, such as those that are critical to vulval morphogenesis. Loss of LIN-12 function results in an egg-laying–defective phenotype (Egl) because of misspecification of several vulval and uterine cell fates (reviewed in Greenwald 2005).

Genetic interactions between Notch signaling components and other cellular processes are uncovering a variety of cellular mechanisms that regulate Notch pathway activity. Both positive and negative modulators have been identified through mutations that alter the amount of Notch signaling activation in animals with mutant Notch receptors (for example, Sundaram and Greenwald 1993; Verheyen *et al.* 1996; Mourikis *et al.* 2010; reviewed in Fortini 2009). Downregulators identified through this approach in *C. elegans* include components of endoplasmic reticulum associated protein degradation (ERAD) (Grant and Greenwald 1996), cargo selectivity for ER-to-Golgi transport (Wen and Greenwald 1999), endocytic trafficking (de Souza *et al.* 2007), and ubiquitin-mediated proteasome degradation (Hubbard *et al.* 1997). The mechanisms of Notch pathway regulation are proving to be functionally conserved, but the relative role of each of these modulating effects is likely to differ for distinct cellular contexts. Notch pathway modulation in *C. elegans* has been well studied in larval and adult signaling events, but little is known about the regulation of Notch activation in the embryo.

SEL-10 was identified as a down regulator of LIN-12 in *C. elegans*, and was shown to act through ubiquitin-mediated proteasomal degradation (Hubbard *et al.* 1997; Wu *et al.* 2001; Li *et al.* 2002). SEL-10 is a member of the family of Fbw7 proteins (F-box and WD repeat domain-containing 7) that includes the yeast and human Cdc4 proteins (reviewed in Welcker and Clurman 2008). The molecular role of Fbw7 proteins, like other F-box proteins, is to provide a substrate recognition domain for the multisubunit SCF (Skp1–Cullin1–F-box) type E3 ubiquitin ligases (Bosu and Kipreos 2008). The substrates that are targeted for ubiquitination by Fbw7 proteins include proteins whose levels must be tightly controlled during cell division and differentiation (*e.g.*, cyclin E, Jun, Myc, and Notch). Loss-of-function mutations in Fbw7 genes are associated with tumorigenesis, as Fbw7 substrates become inappropriately stabilized (Welcker and Clurman 2008). Studies in both *C. elegans* and mammals have established presenilin and the Notch intracellular domain as direct targets of the SEL-10 Fbw7 protein, which promotes their ubiquitination and proteasomal degradation (Hubbard *et al.* 1997; Wu *et al.* 1998; Wu *et al.* 2001; Gupta-Rossi *et al.* 2001; Li *et al.* 2002); however, such a role for SEL-10 in the embryo has not yet been explored. Genetic interactions between *C. elegans sel-10* and genes of the sex-determination pathway point to additional targets of SEL-10–mediated downregulation (Jager *et al.* 2004), making the study of *sel-10* throughout *C. elegans* development a useful model system in which to analyze the dynamic function of Fbw7 proteins.

In this study, we sought to identify cellular components that regulate Notch signaling in the early embryo. We began with a genetically sensitized system that consisted of a mutant form of APH-1, the conserved seven-pass transmembrane protein that is part of the γ-secretase complex. The nonsense allele *aph-1(zu147)* is predicted to encode a truncated APH-1 protein that lacks the C-terminal 33 residues (Goutte *et al.* 2002). These terminal residues are not essential for APH-1 function, as homozygous *aph-1(zu147)* animals are fertile and egg-laying proficient, with only a partially penetrant maternal-effect embryonic lethality. In contrast, stronger *aph-1* mutant alleles cause a fully penetrant Egl phenotype and more severe maternal-effect lethality (Francis *et al.* 2002; Goutte *et al.* 2002). Most embryos from *aph-1(zu147)* hermaphrodites have sufficient APH-1 function to support Notch signaling at the 4-cell stage, but not enough for the 12-cell stage cell interaction (Goutte *et al.* 2002). Thus *aph-1(zu147)* animals provide a highly sensitized platform from which to search for modulators of these early embryonic signaling events. We reasoned that loss-of-function mutations in genes that negatively regulate Notch signaling in the early embryo might compensate for insufficient *aph-1(zu147)* activity, thus allowing a higher proportion of the embryos from *aph-1(zu147)* mothers to survive. We describe here a new gene, *sao-1* (**s**uppressor of **a**ph-**o**ne), that we isolated through such a suppressor screen. Removal of *sao-1* function suppresses the embryonic lethality caused by *aph-1(zu147)* and also shows genetic interactions with mutant forms of *glp-1* and *lag-1*. Using yeast two-hybrid analysis, we demonstrate that the SAO-1 protein interacts with the E3 ubiquitin ligase component SEL-10, suggesting a possible mechanism for *sao-1*–mediated suppression. SAO-1 is a novel protein that contains a GYF domain, an evolutionarily conserved protein–protein interaction domain. Because little functional analysis currently exists for GYF-domain proteins in higher eukaryotes, analysis of the *C. elegans sao-1* gene at the level of mutant phenotype and protein–protein interaction provides a context in which to explore the role of a specific GYF-domain protein in metazoans.

Materials and Methods

Strains and genetic manipulations

All strains were derived from the Bristol N2 strain and maintained according to standard procedures at 20° unless otherwise noted (Brenner 1974). Mutations were supplied by the *Caenorhabditis* Genetics Center (University of Minnesota, Minneapolis, Minnesota) unless noted, and are listed by linkage

group (LG). LGI: *unc-29(e1072)*, *aph-1(zu147*, *zu123)* (J. Priess), *aph-1(or28*, ep140), and *lin-11(n566)*. LGIII: *unc-32(e189)*, *glp-1(q35)* (J. Kimble), *glp-1(e2144*, *e2142)* (J. Priess, see note below), *glp-1(bn18*, ar202), *lin-12(n302*, *n676n930)*. LGIV: *lag-1(om13)*. LGV: *dpy-11(e224)*, *sqt-3 (sc8)*, *lon-3(e2175)*, *sel-10(n1077*, *bc243)* (B. Conradt), *sel-10 (ar41)*, *sao-1(ik1)* (this study), *sao-1(ok3335)* (*C. elegans* Knockout Consortium), *unc-76(e911)*, *itDf2* and *nDf42*. LGX: *sel-12(ar131*, *ar171*, *ty11)* and the balancer *hT2[bli-4(e937) let-?(h661)*] (I;III). For SNP mapping, the wild-type Hawaiian strain CB4856 was used. The following reporter constructs were used for cell identification: *zmp-1*::*gfp* reporter for anchor cells (Wang and Sternberg 2000), *cog-2*::*gfp* reporter for uterine π-cells(Hanna-Rose and Han 1999), and *tph-1*::*gfp* (Sze *et al.* 2000) for hermaphrodite specific neurons (HSNs). The *glp-1(e2144)* allele used here was obtained from the Priess laboratory where it was misreferred to as *glp-1(e2141)* (Dalfó *et al.* 2010); we sequenced our allele to confirm its identity as (*e2144)* (c2785t mutation), and use the corrected nomenclature here.

Suppressor screen: *unc-29(e1072) aph-1(zu147) lin-11 (n566)/hT2* heterozygous hermaphrodites were mutagenized with EMS and allowed to self-fertilize. When the F_2 population had reached the L4 stage, 1 ml of 10 mM levamisole (Sigma; L9756) was added to each plate to enrich for homozygous Unc-29 F_2 individuals; plates were screened 1–2 days later for bags of worms, indicative of high progeny survival. From 10,400 mutagenized haploid genomes, six extragenic mutations, corresponding to four or five genes, were found to dramatically increase the percentage of viable progeny. The *ik1* mutation was outcrossed at least five times before analysis. The deletion allele *ok3335* was generated by the *C. elegans* Knockout Consortium, Oklahoma Medical Research Foundation. We sequenced the *sao-1* gene in homozygous *ok3335* animals and found that 691 bp are deleted within the *sao-1* open reading frame (ORF), including most of exon 1 and all of exons 2, 3, and 4.

Testing the maternal effect of sao-1: To determine whether embryonic *sao-1* genotype plays a role in the survival of *aph-1 (zu147)* embryos, live progeny were collected from partially suppressed *aph-1(zu147)*; *sao-1/+* mothers and their genotype was determined on the basis of the presence of the *dpy-11* marker and on the generation of live progeny in the next generation. In all experiments, homozygous *sao-1* mutant embryos represented ~25% of the live progeny as did homozygous *sao-1*(+) progeny, indicating that the degree of suppression was determined by the maternal genotype rather than the embryonic genotype. For example, the live progeny from *unc-29(e1072) aph-1(zu147)*; *dpy-11(e224) sao-1 (ik1)/+* mothers were 26% Dpy Sao, 26% non-Dpy non-Sao, and 48% heterozygous (n = 77); in a separate experiment, 26% of the live progeny from *unc-29 (e1072) aph-1 (zu147)*; *sao-1(ok3335)/dpy-11(e224)* mothers were homozygous Dpy (n = 2055). Paternal wild-type *sao-1(+)* did not decrease the suppression that maternal *sao-1(ik1)* imposed on *aph-1(zu147)* embryos: hermaphrodites of genotype *unc-29(e1072) aph-1(zu147)*; *dpy-11(e224) sao-1(ik1)* yielded 82% viable self-progeny (n = 496) compared to 80% viable cross-progeny (n = 395, all non-Dpy) after mating to males of genotype *unc-29(e1072) aph-1(zu147)*.

Phenotypic analysis: *aph-1* mutant strains were maintained as heterozygotes with the following genotype: *unc-29 (e1072) aph-1/hT2[bli-4(e937) let-?(h661)]*, and homozygous *aph-1* animals were selected for phenotypic analysis by selecting worms with the Unc-29 phenotype (homozygous *hT2* animals are embryonic lethal due to the *h661* mutation in an unidentified gene). In all cases, test strains were prepared and scored simultaneously with the relevant control strain. Viable progeny were measured by counting eggs laid over a 5- to 8-hr interval, counting the number of unhatched eggs 20–24 hr later and counting the number of viable animals that reached at least the L4 stage after an additional 48–60 hr (times were increased for 15° experiments and decreased for 25° experiments accordingly); eggs were analyzed from a minimum of 10 different mothers for each genotype. Progeny viability was calculated as the proportion of total eggs laid that grew to at least the L4 stage. Hatching rate was calculated as the proportion of embryos that successfully hatch (deduced from the counted number of unhatched embryos). Larval viability was calculated as the proportion of hatched embryos that grew into viable L4/adults. Embryos were observed by Nomarski Microscopy (Zeiss Axioplan) for measurements of embryonic morphogenesis and pharynx formation; the criteria used for scoring an embryo as having successful morphogenesis was the full enclosure by hypodermal cells, regardless of slight abnormal shapes. For temperature-sensitive *glp-1* and *lag-1* alleles, strains were maintained at the permissive temperature until hatching, at which point they were grown at the indicated experimental temperature. For embryonic assessment of strains that are sterile at the restrictive temperature, such as *glp-1(bn18)*, *glp-1(e2144)*, and *glp-1(ar202)*, embryos were obtained by allowing mothers to develop at the permissive temperature until mid L4 stage to allow some germline proliferation; after 12–24 hr of acclimation at the restrictive temperature, embryos were then collected and assayed as above. Sterility was measured by growing strains at the indicated temperature from the time of hatching; individually plated animals were scored as fertile if any embryos were made, and the general appearance of their gonads under brightfield microscopy was noted.

Molecular identification of sao-1

The *ik1* mutation was mapped to chromosome V, at 5.5 m.u. from *dpy-11(e224)* (5/46 *ik1* homozygotes from *ik1/dpy-11* picked up the *dpy-11*). Bristol/Hawaiian recombinants were collected for SNP analysis from the heterozygous strain *sqt-3 (sc8) sao-1(ik1) unc-76(e911)/+* (Hawaiian from CB4856). Sixteen Rol–non-Unc recombinants were identified, and half

of these recombined to the right of *ik1* and half to the left. These 16 recombinants were analyzed with SNPs in the *sqt-3*–*unc-76* region; *ik1* was found to lie between SNP F55B12 [1] and SNP F58E10[3] (3/6 recombinants between SNP F55B12[1] and *ik1*, and 3/6 between *ik1* and SNP F58E10 [3]). Two cosmids map to the center of this 175-kb region: R10D12 and C06B3 (supplied by the Wellcome Trust Sanger Institute, Cambridge, UK). These were injected into *unc-29 (e1072) aph-1(zu147) sao-1(ik1)* worms [as previously described in Goutte *et al.* (2002)] to look for antisuppression. Candidate ORFs within the R10D12 cosmid region were then analyzed by RNAi for the ability to suppress the maternal-effect lethality of *aph-1(zu147)* homozygous animals. A total of 10–15 homozygous *unc-29(e1072) aph-1(zu147)* L4 worms were injected with double stranded RNA corresponding to one of four ORFs: R10D12.2, R10D12.8, R10D12.13, and R10D12.14. Double stranded RNA was generated by run off transcription from T7 binding-site–tagged PCR templates using Ampliscribe T7 High-Yield Transcription kit from Epicentre (primer sequences available upon request) and injected at ~1 μg/μl dsRNA. In the first three cases, *aph-1 (zu147)* worms continued to generate mostly dead embryos; in contrast, worms injected with R10D12.14 RNA yielded a striking number of live progeny, which then grew up to yield live progeny themselves. Two independent cDNAs corresponding to the R10D12.14 ORF were cloned from each of wild-type and *sao-1(ik1)* mutant worms (mixed stage): Total cDNA was generated by RT-PCR using Invitrogen's Superscript III kit and then used as template for PCR with Clonetech Titanium Taq Polymerase using SL1 and SL2 primers (Spieth *et al.* 1993) in combination with a primer that overlaps the predicted stop codon of R10D12.14 (primer sequences available upon request). In both cases, products were identified with the spliced leader sequence SL2, but not with SL1. Sequence analysis of these four independent cDNA clones confirmed the intron/exon junctions predicted by Genefinder and confirmed by ESTs identified for the R10D12.14 ORF (http://wormbase.org). Genefinder predicts four versions of spliced R10D12.14 products, termed a–d; our sequences correspond to R10D12.14a, containing six exons. The only difference between the wild-type and the *ik1* coding region of R10D12.14 was a single nucleotide change that results in a Leu-to-Phe change at predicted amino acid 59 (codon CTT to TTT).

Yeast two-hybrid analysis

The LexA-based yeast two-hybrid system with dual reporters (*lacZ* and *HIS3*) was used (Hollenberg *et al.* 1995). Yeast strains, AMR70 and L40, and plasmids for building fusion constructs were supplied by Peter Pryciak: pGAD-XP for activation domain fusions and pBTM116 for DNA binding domain fusions (Pryciak and Hartwell 1996). cDNA for *sel-10* was provided by Jane Hubbard and Iva Greenwald. *lin-23* cDNA was provided by Oliver Hobert. cDNA sequences were PCR amplified using primers that introduced an *Xma*I restriction site at the 5′ end of a protein coding region or a *Sal*I resriction site at the 3′ end of the region (primer sequences available upon request). Restricted fragments were ligated into *Xma*I–*Sal*I cut pGAD-XP or pBTM116. All AD constructs were transformed into L40, and all DBD constructs were transformed into AMR70; desired pairwise combinations were created by mating transformants and selecting for doubly transformed diploids for analysis. *HIS3* expression was analyzed by growing on −HIS solid medium supplemented with 0.25 M or 1.25 M 3-aminotriazole. Liquid β-galacatosidase assays were carried out according to standard procedures (Pryciak and Hartwell 1996). Yeast extracts were made from exponentially growing cultures of the diploid strains used in *lacZ* assays, using the procedure of Kushnirov (2000). Cell lysate concentrations were equalized according to OD_{600} culture measurements and equal volumes were fractionated on 10–12% polyacrylamide Tris/glycine gels. Western blot analysis was performed using antibodies against the Gal4 activation domain (Millipore; 06-283), the LexA DNA binding domain (Millipore; 06-719), and the yeast Cdc28 protein (Santa Cruz Biotech; sc-6709) as a control for protein levels in different yeast extracts. Chemicrome (TM) molecular weight markers (Sigma) were used for size standards. Extracts of yeast strains expressing SAO-1(+) and SAO-1(ik1) fusions were compared in >10 independently prepared extracts, some from haploid cells expressing only the SAO-1 AD fusion construct, and some from diploid cells expressing the SAO-1 AD fusion as well as a SEL-10 DBD fusion (as shown in Figure 3C); although there was some strain-independent variability from extract to extract, there was no consistent difference between SAO-1(+) and SAO-1(ik1) fusion proteins.

Results

We isolated six extragenic mutations in a screen for suppression of *aph-1(zu147)* maternal-effect lethality (*Materials and Methods*) and present here our analysis of one of these mutations, *ik1*, and the novel gene it defines, *sao-1* (suppressor of aph-one). We also obtained from the *C. elegans* Gene Knockout Consortium the deletion allele *sao-1(ok3335)* and include this mutation in our analysis of *sao-1* function.

Reduced sao-1 activity suppresses aph-1(zu147) embryonic lethality

The partial loss-of-function allele *aph-1(zu147)* causes an incompletely penetrant maternal-effect embryonic lethality: almost all progeny produced by an *aph-1(zu147)* hermaphrodite arrest as late-stage embryos or hatchlings with the hallmark Notch phenotype of a missing anterior pharynx, indicating failed Notch signaling at the 12-cell stage (Figure 1A and Goutte *et al.* 2002; Priess 2005). In sharp contrast, *aph-1 (zu147)*; *sao-1(ik1)* homozygous worms produce virtually all viable progeny (Table 1). Suppression of the *aph-1(zu147)* embryonic defect is equally dramatic with the deletion allele *sao-1(ok3335)* (described below) and by *sao-1* RNAi (Table 1 and Figure 1B), indicating that the Notch defect of *aph-1 (zu147)* embryos is overcome by removing *sao-1* wild-type function. Partial suppression is observed in animals that are

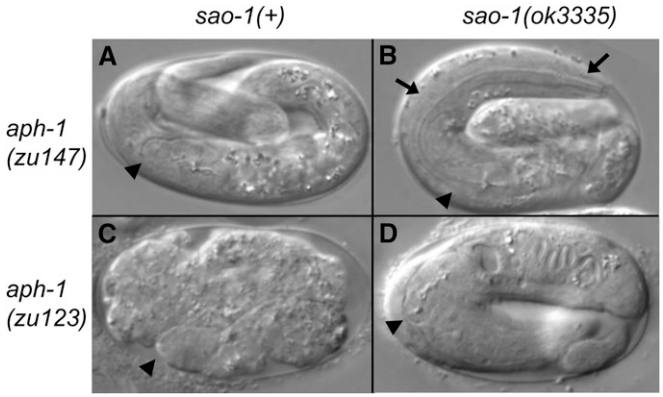

Figure 1 sao-1(ok3335) suppresses aph-1(zu147) and aph-1(zu123). Representative terminal stage embryos viewed by light microscopy; arrowhead indicates posterior pharynx and arrows indicate anterior pharynx if present; embryos are oriented posterior to the right and collected from mothers with the following genotypes: (A) *unc-29(e1072) aph-1(zu147)*; (B) *unc-29(e1072) aph-1(zu147); sao-1(ok3335)*; (C) *unc-29(e1072) aph-1 (zu123)*; and (D) *unc-29(e1072) aph-1(zu123); sao-1(ok3335)*. The embryo shown in C has failed to undergo body morphogenesis; instead of fully enclosing the embryo, the hypodermal cells are clumped on one side, leaving the posterior pharynx exposed on the other side of the embryo. See Table 2 for the frequency of these phenotypes among embryos.

heterozygous for either *sao-1(ik1)*, *sao-1(ok3335)*, or the chromosomal deletion *itDf2* (Table 1). These results suggest that the *sao-1* locus is haploinsufficient, such that even a small reduction in *sao-1* function is effective at *aph-1(zu147)* suppression. The *sao-1(ik1)* allele must retain some low level of *sao-1* activity because suppression in *sao-1(ik1)* heterozygotes is not as strong as in deletion heterozygotes (Table 1). Analysis of embryos from *sao-1* heterozygous animals establishes that it is maternal rather than zygotic *sao-1* activity that influences embryonic survival (*Materials and Methods*). Taken together these genetic analyses suggest that the SAO-1 protein has a negative effect on *aph-1(zu147)* activity in the early embryo.

More severe alleles of *aph-1* (*zu123*, *or28*, and *ep140*) cause fully penetrant embryonic lethality in which the embryos not only lack an anterior pharynx (due to failed Notch signaling at the 12-cell stage), but also fail to complete body morphogenesis because of failed Notch signaling at the 4-cell stage (Figure 1C and Goutte *et al.* 2002; Priess 2005). Neither *sao-1(ik1)* nor *sao-1(ok3335)* can restore embryonic viability to these *aph-1* mutants (data not shown). However, the *sao-1(ok3335)* mutant background allows improved body morphogenesis for the weakest of these alleles, *aph-1 (zu123)* (Figure 1D and Table 2), which is not completely devoid of *aph-1* activity (Goutte *et al.* 2002). Although some *aph-1(zu123) sao-1(ok3335)* embryos exhibit successful body morphogenesis, none of these embryos induces an anterior pharynx, indicative of persisting Notch signaling defects at the 12-cell stage ($n = 94$). Thus, removing *sao-1* activity appears to increase Notch signaling activity in early *aph-1(zu123)* embryos to allow some successful Notch signaling at the 4-cell stage, but not to levels that are sufficient for all Notch signaling events required for embryonic viability. Collectively, our results suggest that reducing *sao-1* function can elevate Notch signaling in embryos with decreased but not entirely absent *aph-1* activity.

Table 1 Reduction of *sao-1* activity suppresses *aph-1(zu147)* embryonic lethality

Genotype of mother	% viable progeny (*n*)
aph-1(zu147)	1.2 (1835)
aph-1(zu147); sao-1(ik1)	99 (1645)
aph-1(zu147); sao-1(ok3335)	97 (1105)
aph-1(zu147); sao-1(RNAi)[a]	99 (1210)
aph-1(zu147); sao-1(ik1)/itDf2	98 (1758)[b]
aph-1(zu147); sao-1(ik1)/+[c]	22 (3381)
aph-1(zu147); sao-1(ok3335)/+[c]	53 (3901)
aph-1(zu147); itDf2/+	50 (3623)[b]

Embryos were collected from at least 10 mothers of the indicated genotype; all animals were also homozygous for *unc-29(e1072)*. Viable progeny are those that reach at least the L4 stage. n, number of embryos scored.

[a] Embryos were collected 16 hr after injection of L4s (see *Materials and Methods*).

[b] Percentage of viability was calculated after subtracting the expected one-quarter inviable homozygous *itDf2* progeny; see Figure 2 for *itDf2* location.

[c] Actual genotype: *unc-29(e2072) aph-1(zu147); sao-1(ik1* or *ok3335)/dpy-11 (e224)*; embryos of different genotypes [*dpy-11(e224)* or *dpy-11(e224)/sao-1* or *sao-1*] had similar survival rates (see *Materials and Methods*).

In an otherwise wild-type background, *sao-1(ik1)* and *sao-1(ok3335)* do not cause visible deleterious effects under standard growth conditions. However, we observe several incompletely penetrant phenotypes among animals that are homozygous for the deletion allele *sao-1(ok3335)* and raised at the elevated temperature of 25°. These include embryonic lethality (bottom row of Table 3), reduced brood size, egg retention, and increased incidence of males (data not shown). These phenotypes are likely to be associated with removal of *sao-1* function because we were unable to segregate them away from the *aph-1* suppression phenotype of *sao-1(ok3335)* after 13 rounds of outcrossing, including two recombination events within a 1.5 m.u. distance on each side of *sao-1(ok3335)*. Furthermore, we note that the independently isolated *ik1* allele also exhibits a very low, though significant embryonic lethality at 25° and even more at 27° (bottom row of Table 3 and data not shown). The existence of these phenotypes at high temperatures indicates that *sao-1* function is not essential under normal growth conditions, but its activity may become critical upon stress; the specific nature of these phenotypes is being investigated separately.

sao-1(ik1) suppresses a mutation in the Notch downstream effector lag-1

To probe the specificity of *sao-1* function, we asked whether *sao-1* mutations could influence Notch signaling when components other than *aph-1* were compromised. The downstream Notch transcriptional effector LAG-1 is partially inactivated by the temperature-sensitive mutation *lag-1 (om13)*, which introduces a single amino acid change (A551T) (D. Greenstein, personal communication) and causes incompletely penetrant Notch signaling defects in both early and late embryogenesis (Qiao *et al.* 1995). At

Table 2 *sao-1(ok3335)* suppresses embryonic morphogenesis defect of weak *aph-1 alleles*

	% embryos with successful body morphogenesis (*n*)	
Genotype of mother	*sao-1(+)*	*sao-1(ok3335)*
aph-1(zu147)	89 (767)	97 (325)
aph-1(zu123)	0.82 (968)	20 (712)
aph-1(ep140)	0 (401)	0 (445)
aph-1(or28)	0 (315)	0 (452)

Embryos were collected from at least 10 mothers that were homozygous for either *sao-1(+)* or *sao-1(ok3335)* and also homozygous for the indicated *aph-1* allele; all animals were also homozygous for *unc-29(e1072)*. *n*, number of embryos scored. Embryos were scored as having successful body morphogenesis if the hypodermis successfully enclosed the embryo and elongation proceeded; see Figure 1 for representative embryos.

the restrictive temperatures of 20° or 25°, roughly half of the embryos from *lag-1(om13)* mothers are defective in early Notch signaling events and thus fail to hatch. The remainder of the embryos are successful in these early events, but fail in later embryonic Notch signaling events that drive formation of the head, the excretory cell, the anus, and the rectum; hence these embryos hatch but arrest as larvae (Lambie and Kimble 1991; Qiao *et al.* 1995). We found that the survival of progeny from *lag-1(om13)* hermaphrodites is significantly improved in a *sao-1(ik1)* mutant background (Table 3). The overall increase in viability is the combined result of a small increase in hatching rate and a large increase in larval viability. For example, at 25°, 54% of *lag-1(om13)* embryos hatch *vs.* 63% of *lag-1(om13)*; *sao-1(ik1)* embryos (this difference is significant according to a two-tailed Fisher exact test: *P* value <0.0001, see Table 3 for *n* values) and 7.3% of *lag-1(om13)* hatchlings are viable compared to 33% of *lag-1(om13)*; *sao-1(ik1)* hatchlings (significant difference according to a two-tailed Fisher exact test: *P* value <0.0001, $n = 697$ and $n = 543$, respectively). The suppression of both embryonic and larval lethality suggests that *sao-1* influences both early and late embryonic Notch signaling events. We do not observe a similar improvement of *lag-1(om13)* viability in the *sao-1(ok3335)* mutant background, though assessment at 25° could not be easily interpreted due to temperature-sensitive lethality introduced by the *sao-1(ok3335)* allele at this temperature (Table 3 and see next section). The genetic interaction between *sao-1(ik1)* and *lag-1(om13)* suggests that *sao-1* activity downregulates Notch signaling, even in an *aph-1(+)* background.

sao-1 influences signaling capacity of altered GLP-1 receptors during embryogenesis

Mutant GLP-1 receptors were tested for sensitivity to *sao-1* activity in the early embryo. We analyzed the effect of three loss-of-function (lf) alleles (*e2142*, *e2144*, and *bn18*) (Priess *et al.* 1987; Kodoyianni *et al.* 1992) and one hyperactive allele (*ar202*) (Pepper *et al.* 2003). Alone, each of these temperature-sensitive mutations causes embryonic lethality at its restrictive temperature, indicating that insufficient or excessive GLP-1 activity disrupts embryogenesis (Priess *et al.*

Table 3 Interaction of *sao-1* with *lag-1* and *glp-1* embryonic mutants

		% viable progeny (*n*)		
Genotype of mother	Temperature	*sao-1(+)*	*sao-1(ik1)*	*sao-1(ok3335)*
lag-1(om13)[a]	20°	4.4 (480)	30 (502)**	4.2 (1116)
	25°	4.0 (1289)	20 (868)**	0.66 (911)**
glp-1(e2144)[a]	15°	100 (161)	99 (282)	99 (928)
	20°	99 (881)	97 (800)*	41 (392)**
	23°	3.2 (693)	1.3 (634)	0 (430)**
	25°	0 (238)	0 (468)	0 (253)
glp-1(e2142)[a]	15°	94 (599)	89 (555)*	38 (445)**
	20°	14 (273)	2.8 (324)**	0 (306)**
	25°	0 (262)	0 (246)	0 (>500)
glp-1(bn18)[a]	20°	93 (580)	84 (365)**	17 (544)**
	23°	6.2 (499)	0 (477)**	0 (>500)**
	25°	0 (>500)	0 (>500)	0 (>500)
glp-1(ar202)[a]	20°	80 (426)	90 (479)**	47 (403)**
	23°	68 (989)	70 (735)	22 (446)**
+	15°	100 (275)	100 (761)	99 (1044)
	20°	100 (288)	99 (718)	98 (588)
	23°	100 (309)	99 (873)	93 (1341)**
	25°	99 (569)	97 (646)*	60 (882)**

Embryos were collected from at least 10 mothers that were homozygous for either *sao-1(+)*, *sao-1(ik1)* or *sao-1(ok3335)* and also homozygous for the indicated *glp-1* or *lag-1* allele; mothers represented in the last four rows have no mutation other than the indicated *sao-1* allele. Mothers were raised at 20 °, shifted to the designated temperature as mid L4s, and acclimated for at least 24 hr before embryos were collected and raised at the same temperature (see *Materials and Methods* for details). Viable progeny are those that reach at least the L4 stage. *n*, number of embryos scored. A two-tailed Fisher exact test was performed for each *sao-1(ik1)* or *sao-1(ok3335)* value relative to the equivalent *sao-1(+)* value in the same row; asterisks indicate a statistically significant difference between the *sao-1* mutant and the corresponding *sao-1(+)* embryos with *P* values as follows: $*P < 0.01$, $**P < 0.0001$.

[a] Temperature-sensitive alleles for which 25 ° is the restrictive temperature at which embryonic viability is severely compromised (Priess *et al.* 1987; Kodoyianni *et al.* 1992; Qiao *et al.* 1995; Pepper *et al.* 2003).

Table 4 *sao-1* mutations increase *glp-1* activity in the germ line

Genotype of mother	Temperature	% fertile animals (*n*)		
		sao-1(+)	*sao-1(ik1)*	*sao-1(ok3335)*
glp-1(q35)[a]	20°	0.9 (222)	8.6 (233)*	52 (266)*
	23°	13 (208)	99 (162)*	98 (262)*
glp-1(bn18)[b]	20°	98 (122)	100 (>500)	99 (197)
	23°	31 (325)	50 (161)*	80 (215)*
	25°	0 (>500)	0 (>500)	0 (>500)
glp-1(e2144)[b]	20°	100 (100)	100 (202)	99 (524)
	23°	0 (105)	0 (105)	3.4 (179)
	25°	0 (>500)	0 (>500)	0 (>500)
glp-1(ar202)[b,c]	20°	98 (204)	95 (190)	85 (213)*
+	20°	ND	100 (>500)	100 (>500)
	23°	ND	100 (203)	100 (322)
	25°	ND	100 (324)	99 (193)

Hermaphrodites that were homozygous for either *sao-1(+)*, *sao-1(ik1)* or *sao-1(ok3335)* and also homozygous for the indicated *glp-1* allele were raised at the specified temperature and scored for fertility; the last four rows represent animals with no mutation other than the indicated *sao-1* allele. Animals that generated any embryos were scored as fertile. *n*, number of animals scored. ND, not determined. A two-tailed Fisher exact test was performed on each *sao-1(ik1)* or *sao-1(ok3335)* value relative to the equivalent *sao-1(+)* value in the same row; an asterisk indicates a difference between the wild-type and *sao-1* mutant that is statistically significant with a *P* value <0.0001.

[a] The *glp-1(q35)* allele causes a loss-of-function germline phenotype that is cold sensitive: animals are fertile at 25 °, but sterile at 15 ° (Mango *et al.* 1991). Full genotype: *unc-32(e189) glp-1(q35)*.

[b] Temperature-sensitive *glp-1* alleles for which 25 ° is the restrictive temperature at which virtually all animals are sterile (Priess *et al.* 1987; Kodoyianni *et al.* 1992; Pepper *et al.* 2003).

[c] Fertile animals differed in appearance of gonads: for example aberrant gonads were visible under the dissecting microscope in 17% of the fertile *glp-1(ar202)* mutants (n = 201) *vs.* 71% of the fertile *glp-1(ar202); sao-1(ok3335)* double mutants (n = 182); such gonad abnormalities were not observed among the *sao-1(ok3335)* single mutants.

1987; Kodoyianni *et al.* 1992; Hutter and Schnabel 1994; Berry *et al.* 1997; Pepper *et al.* 2003). We found that *sao-1* mutations significantly increased the degree of embryonic lethality observed in all four *glp-1* mutants at permissive or semipermissive temperatures (Table 3). These genetic interactions clearly point to an effect of *sao-1* function on GLP-1 signaling ability. However, the direction of this effect (*i.e.*, positive or negative) is unclear for several reasons: First, embryonic lethality can result from insufficient Notch signaling as well as from ectopic Notch signaling, or even from a combination of these effects at different embryonic stages, since there are at least six distinct cell-fate choices in the embryo that depend upon the proper balance of Notch-induced and uninduced cells (Priess 2005). Second, the fact that both *lf* and hyperactive *glp-1* alleles cause more embryonic lethality in *sao-1*–deficient embryos prevents a simple interpretation of embryonic lethality, and instead points to the complexity of properly regulating GLP-1 activity in the embryo. Third, interpretation of *glp-1(lf)*; *sao-1* double mutants is complicated by the existence of LIN-12 receptor that can mediate some embryonic Notch signaling in the absence of GLP-1, and whose expression is normally repressed in Notch-induced embryonic cells (Neves and Priess 2005). Decreased GLP-1 activity in early embryonic interactions has been shown to derepress *lin-12* and other Notch signaling component genes; the effect of such inappropriately expressed LIN-12 could be exacerbated by the removal of a downregulator of Notch signaling, together causing ectopic Notch activation in subsequent cells (see *Discussion* for another possibility). Fourth, the phenotype of the arrested embryos from *glp-1(lf)*; *sao-1* double mutants is variable, with some embryos resembling *glp-1*–deficient embryos, some embryos resembling *glp-1 lin-12*–deficient embryos, and others exhibiting less distinct phenotypes (unpublished observations), suggesting that a variety of specific causes for embryonic lethality exists in these double mutants. Because of these considerations, the increased embryonic lethality in *glp-1*; *sao-1* double mutants cannot be used to infer whether the effect of SAO-1 on individual Notch signaling events in the embryo is positive or negative. To more decisively characterize the effect of *sao-1* mutations on mutant GLP-1 receptor activity, we analyzed germline development.

Reduced sao-1 activity increases GLP-1 receptor signaling during germline development

GLP-1 activation induces germ cell proliferation throughout larval and adult life, and the extent of germline proliferation serves as a direct readout of GLP-1 activity; even partial increases in GLP-1 signaling can cause measurable fertility in an otherwise sterile GLP-1–deficient animal (Kimble and Crittenden 2005). The partial loss-of-function *glp-1* alleles *bn18*, *q35*, and *e2144* fail to promote germline proliferation at restrictive temperatures, resulting in 100% sterile animals, while at intermediate temperatures they retain some function and produce a small number of fertile animals (Priess *et al.* 1987; Mango *et al.* 1991; Kodoyianni *et al.* 1992). We found that when *sao-1* activity is eliminated, a greater percentage of these *glp-1* mutant animals achieve fertility (Table 4). Furthermore, fertile *glp-1*; *sao-1* double mutants have larger brood sizes than fertile *glp-1* single mutants. For example, the percentage of fertile animals that generate >100 embryos at 23° is only 1.9% for *glp-1(bn18)* (n = 107) but is increased to 9.1% for *glp-1(bn18)*; *sao-1(ik1)* (n = 55; this difference is significant according to a two-

tailed Fisher exact test, with a P value <0.05). These results suggest that SAO-1 activity antagonizes GLP-1 signaling in the germline. No suppression of *glp-1* sterility was seen at the fully restrictive temperature, indicating that removal of SAO-1 function elevates but does not bypass GLP-1 activity.

The temperature-sensitive hyperactive allele *glp-1(ar202)* also decreases fertility, but it does so because Notch signaling in the germ line is ectopically activated rather than decreased. At elevated temperatures, *glp-1(ar202)* animals have excess germ cell proliferation at the expense of germ cell differentiation (Pepper *et al.* 2003). If SAO-1 downregulates GLP-1 signaling, then removing SAO-1 activity would be predicted to exacerbate the *glp-1(ar202)* germline defects. Indeed, at the permissive temperature of 20°, where virtually all *glp-1 (ar202)* animals are fertile, 15% of *glp-1(ar202)*; *sao-1 (ok3335)* double mutants are completely sterile, and even the fertile animals appear to have aberrant germ lines (Table 4). The fertile *glp-1(ar202)*; *sao-1(ok3335)* double mutants have small brood sizes averaging only 50.6 progeny (± 25.7 SD; n = 31) compared to an average of 151 progeny (± 63.6 SD; n = 20) for single *glp-1(ar202)* animals. To further compare the effect of the *glp-1(ar202)* mutation in the *sao-1(+) vs.* the *sao-1(ok3335)* background, we examined the distribution of mitotic germ cell nuclei throughout the gonads by DAPI staining, and scored the number of gonad arms that displayed either of the two most severe phenotypes associated with ectopic GLP-1 signaling: a tumorous germ line (Tum), in which the entire gonad arm is filled with mitotic nuclei, or proximal mitosis (Pro), in which the proximal end of the gonad is filled with mitotic nuclei rather than differentiated germ cells (Berry *et al.* 1997; Pepper *et al.* 2003). The percentage of gonad arms that display either phenotype at 20° is significantly greater for the *glp-1(ar202)*; *sao-1(ok3335)* double mutants (37%, n = 452 gonad arms) than for the *glp-1(ar202)* single mutants (20%, n = 408 gonad arms; statistically significant difference by two-tailed Fisher exact test: P value <0.0001). Thus by several accounts the effect of the *glp-1(ar202)* mutation, which increases GLP-1 activity in the germ line, appears to be more severe when SAO-1 activity is eliminated, supporting the model that SAO-1 activity downregulates GLP-1–dependent signaling in the germ line.

The second *C. elegans* Notch receptor, LIN-12, is predominantly involved in somatic cell fate decisions in the late embryo and larval stages. Using well-described roles of LIN-12 in vulval development, we searched for evidence of genetic interactions between *sao-1* mutations and weak *lin-12* loss-of-function mutations or gain-of-function mutations, but found no significant effects: *i.e.*, lowering *sao-1* activity did not influence the success of anchor cell (AC) specification or alter the overall egg laying ability of worms with either lowered or elevated *lin-12* activity (Supporting Information, Table S1). The lack of genetic interactions between *sao-1* and *lin-12* is a notable contrast to the readily observed interactions between *sao-1* and *glp-1*. This distinction may reflect a difference in downregulation mechanisms for GLP-1 *vs.* LIN-12 signaling or differences between germline and somatic tissues (*e.g.*, in terms of either *sao-1* expression or the regulation of Notch signaling).

sao-1 encodes a novel GYF-domain protein

We determined the molecular identity of the *sao-1* gene through a combination of SNP mapping, cosmid rescue, and RNAi analysis. Genetic mapping with visible markers and SNP markers localized the *sao-1* gene to a region of 175 kb on chromosome V, flanked by SNP F55B12[1] and SNP F58E10 [3] (Figure 2A). Cosmids from this region were then tested for their ability to supply functional *sao-1* activity by injecting them into *aph-1(zu147)*; *sao-1(ik1)* hermaphrodites and scoring for transgenic rescue of the *sao-1(ik1)* phenotype ("anti-suppression"), as evidenced by dead embryos. A small number of transgenic worms carrying cosmid R10D12 gave 30–50% dead embryos. Candidate ORFs within the R10D12 cosmid region were then analyzed by RNAi for the ability to suppress the maternal-effect lethality of *aph-1(zu147)* homozygous animals. Worms injected with dsRNA corresponding to ORF R10D12.14 yielded a striking number of live progeny (Table 1) in contrast to uninjected worms or worms injected with dsRNA from other ORFs in the region (data not shown).

The identity of R10D12.14 as the *sao-1* ORF was confirmed by the identification of a single nucleotide change in two R10D12.14 cDNAs independently isolated by RT–PCR from *sao-1(ik1)* worms (*Materials and Methods*). Our cDNA analysis is consistent with the predictions of Genefinder for R10D12.14a, and predicts that the *sao-1* gene product is a novel 224-amino-acid protein, whose sequence is shown in Figure 2B. The *sao-1(ok3335)* allele has an internal deletion that removes most of the coding region (*Materials and Methods*). In the *C. elegans* topographical expression map, the expression of R10D12.14 is classified as germ line-enriched and is found in the same expression profile cluster as *aph-1* and *aph-2*; namely, within Mountain 2 (Reinke *et al.* 2000; Kim *et al.* 2001).

The predicted SAO-1 protein contains a GYF domain, a motif that mediates protein–protein interactions and is a member of the general class of protein motifs that bind proline-rich sequences (Kofler and Freund 2006). The GYF domain is characterized by a signature set of conserved aromatic amino acid residues precisely placed to stack between a single α-helix and a small β-sheet. The GYF domain of SAO-1 contains 9 of the 10 signature residues of GYF domains (Figure 2C). Additional features have been used to subcategorize GYF domains into two classes: the SMY2 subfamily and the CDC2BP subfamily (Kofler and Freund 2006). The SAO-1 GYF domain more closely resembles the SMY2 class because of the tight spacing between the first and second predicted β-strands, a hallmark of SMY2-type GYF domains. Within the SMY2 subfamily, SAO-1 and a subset of proteins, including human GIGYF1 and GIGYF 2, show further conservation of GYF-domain sequences lying downstream of the 10 signature residues (Figure 2C). Notably, one of these conserved

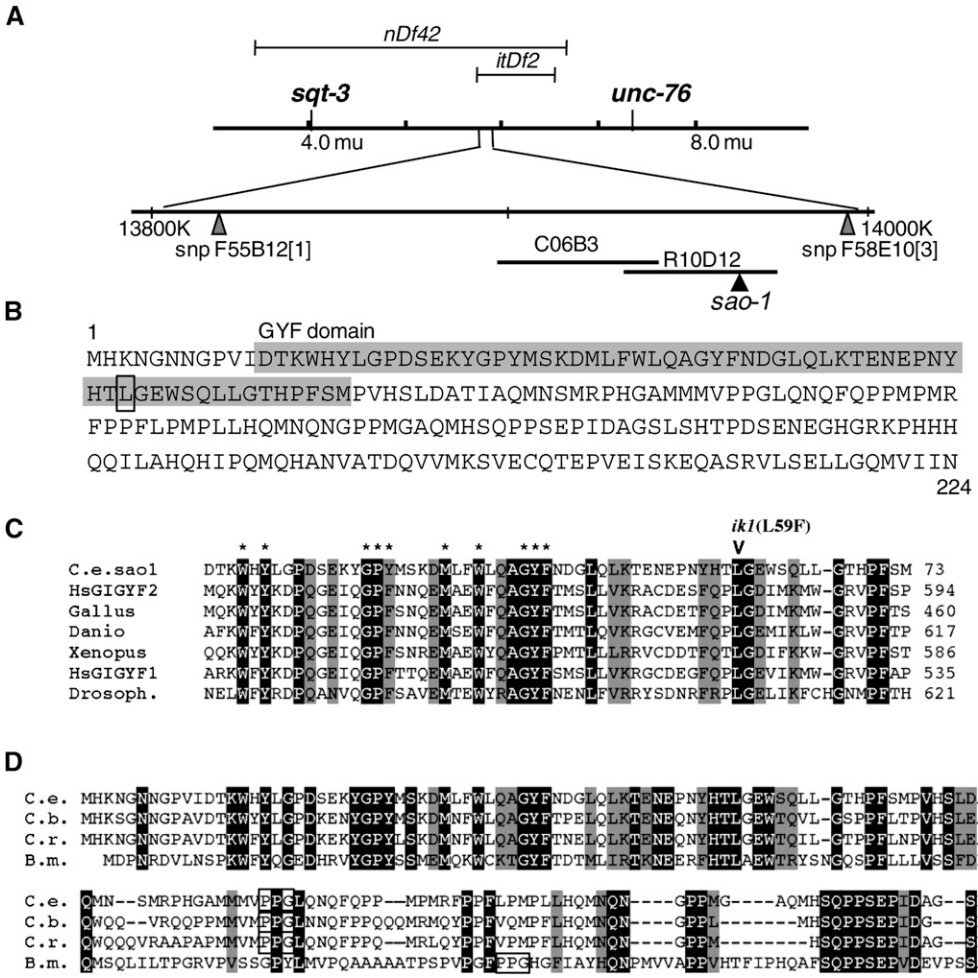

Figure 2 *sao-1* gene locus and protein sequence. (A) Schematic representation of *sao-1* position on chromosome V and the relevant chromosomal deletions (*nDf42* and *itDf2* that remove the *sao-1* locus), cosmids (C06B3 and R10D12), and SNPs (F58E10[3] is position V:13994498 and F55B12[1] is position V:13819498) that are mentioned in the text. (B) Predicted protein sequence of SAO-1 with GYF domain shaded and a box around the residue that is altered by the *ik1* mutation. (C) Alignment of SAO-1 GYF domain with most related GYF domains from other species: *Homo sapiens* NP001096618 GRB10 interacting GYF protein2 (GIGYF2), *Gallus gallus* AAB66717, *Danio rerio* NP001025332, *Xenopus laevis* AAH77291, *Homo sapiens* AAI29992 GRB10 interacting GYF protein1 (GIGYF1), and *Drosophila melanogaster* NP651950. Ten asterisks correspond to hallmark GYF-domain residues (Kofler and Freund 2006); the eighth residue of the SAO-1 GYF domain (Gly19) does not match the hallmark aspartic acid of the SMY2 class nor the hallmark tryptophan of the CD2BP2 class. *sao-1(ik1)* missense mutation is indicated above the SAO-1 sequence. (D) Alignment of *C. elegans* SAO-1 with orthologs from other nematode species shows conservation around GYF domain as well as beyond: CBG11416 from *C. briggsae*, CRE05454 from *C. remanei*, and A8NHL5 from *Brugia malayi*. Occurrences of PPG sequences are boxed. Identical residues are indicated in white on black, and conserved residues in black on gray. Sequence alignments were performed with ClustalW (www.clustal.org) and adjusted by hand.

residues, leucine 59, is the residue that is altered in the *sao-1 (ik1)* mutation (L59F).

The C-terminal portion of SAO-1 has no discernible protein motifs or regions of conservation across the animal kingdom, but among nematode species, sequence conservation beyond the GYF domain reveals putative *sao-1* orthologs (Figure 2D). Given the ability of GYF domains to bind proline-rich sequences, it is notable that the SAO-1 C terminus is enriched in prolines, and in each of the predicted related nematode proteins, the C terminus contains a PPG sequence (Figure 2D), which is the core recognition sequence for GYF domains (Kofler *et al.* 2005). Furthermore, the PPG sequence of SAO-1 is followed by a leucine, consistent with the preferred binding site established for SMY2-type GYF domains, while those of the CD2BP class prefer PPGR/K (Kofler *et al.* 2005). The presence of a putative GYF recognition motif in the C-terminal half of SAO-1 is suggestive of homotypic or intramolecular interactions.

SAO-1 protein interacts directly with the Fbw7 protein SEL-10

In genome-wide yeast two-hybrid analyses, the R10D12.14 ORF (*sao-1*) was found as 1 of 7 proteins that interact with SEL-10, an E3 ubiquitin ligase component, and 1 of 19 proteins that interact with dynein light chain 1 (DLC-1) (Walhout *et al.* 2000; Li *et al.* 2004). These interactions may be pertinent to SAO-1's influence on Notch signaling. We investigated the interaction with SEL-10 because of its established role as

a downregulator of the Notch signaling pathway in *C. elegans* and mammals (Hubbard *et al.* 1997; Wu *et al.* 1998, 2001; Li *et al.* 2002). The N-terminal domain of SEL-10 contains an F-box motif that interacts with the core of the SCF ubiquitin ligase complex, while the C-terminal WD40 repeat domain provides substrate recognition specificity for the complex (Petroski and Deshaies 2005). We generated SAO-1 and SEL-10 yeast two-hybrid constructs to examine the ability of these two proteins to interact (see Figure 3, B, C, and F for protein expression in yeast). A strong interaction between SAO-1 and SEL-10 is detected by expression of a HIS3 reporter (HIS growth assay, data not shown) and a *lacZ* reporter (β-galactosidase activity assay, Figure 3A). By testing the F-box and the WD40 domains of SEL-10 separately, we found that the WD40 domain is sufficient to interact with SAO-1, and a single missense mutation in the eighth WD40 repeat of SEL-10 (G567E) (Jager *et al.* 2004) disrupts this interaction (Figure 3A). The G567E substitution may directly interfere with SAO-1–SEL-10 interaction or it may indirectly prevent SAO-1 interaction by disrupting SEL-10 dimerization (Killian *et al.* 2008). The SAO-1 interaction appears specific for the WD40 domain from SEL-10, as we did not detect an interaction with the WD40 domain from another *C. elegans* Fbw7 protein, LIN-23 (data not shown).

To address whether the SAO-1–SEL-10 interaction is relevant to the *sao-1(ik1)* suppression of *aph-1(zu147)*, we introduced the *ik1* mutation (L59F) into the SAO-1 yeast two-hybrid construct. The *ik1* mutation does not disrupt expression or stability of the SAO-1 fusion protein in yeast (Figure 3C), but dramatically decreases the amount of detectable interaction with SEL-10 (Figure 3A). A similar decrease in interaction is observed when the isolated WD40 domain of SEL-10 is tested against SAO-1(L59F) *vs.* wild-type SAO-1 (Figure 3A). These results raise the possibility that interaction between SAO-1 and SEL-10 contributes to negative regulation of Notch signaling.

The N-terminal region of SAO-1 contains the GYF domain (residues 12–73), while the C terminal two-thirds (residues 74–224) of the protein are nondescript. Despite the fact that SEL-10 binding was disrupted by the *ik1*(L59F) mutation, which resides in the GYF domain of SAO-1, we found that it was actually the C-terminal portion of SAO-1 that mediates SEL-10 binding (Figure 3D). Constructs expressing only the C-terminal 145 or 174 residues of SAO-1 were sufficient to interact with intact SEL-10 or its WD40 domain alone (Figure 3D). Furthermore, the L59F mutation had no effect on SEL-10 binding unless the SAO-1 GYF domain was intact. Therefore, our data suggest that SEL-10 recognition is mediated primarily by the SAO-1 C-terminal domain, but that the N-terminal GYF domain can modulate the SEL-10–SAO-1 interaction in a way that is affected by the *sao-1(ik1)* L59F mutation. It is conceivable that the L59F mutation enhances an intramolecular interaction that masks the SEL-10 binding site in SAO-1 (*Discussion*). In summary, our yeast two-hybrid analysis demonstrates a specific interaction between SAO-1 and SEL-10 that is disrupted by the *sao-1(ik1)* point mutation that we isolated as a suppressor of *aph-1(zu147)*.

A sel-10 mutation can partially suppress aph-1(zu147) embryonic lethality

The physical interaction between SAO-1 and SEL-10 led us to ask whether disrupting *sel-10* function in the embryo might have a similar effect as removing *sao-1* function; namely, suppression of *aph-1(zu147)* embryonic lethality. Two *sel-10* loss-of-function mutations were tested: *bc243* is a null allele (Jager *et al.* 2004) and *ar41* is a strong loss-of-function allele that retains some residual activity (Hubbard *et al.* 1997). Neither *sel-10(bc243)* nor *sel-10(ar41)* was found to suppress *aph-1(zu147)* embryonic lethality (Table 5). Given that these *sel-10* mutations elevate Notch signaling during vulval development (Hubbard *et al.* 1997) and germline development (Pepper *et al.* 2003), our results suggest a different scenario in the embryo: either sel-10 does not downregulate Notch signaling or it may do so redundantly with other proteins. We then tested the *sel-10(n1077)* allele, which causes the single amino acid substitution G567E tested in our yeast two-hybrid analysis. This mutation has been shown to prevent SEL-10 function and also cause a dominant negative phenotype in which the SEL-10 (G567E) protein is thought to interfere with the function of other redundant SCF F-box components (Jager *et al.* 2004). Interestingly, the *sel-10(n1077)* allele is able to partially suppress *aph-1(zu147)* embryonic lethality (Table 5). The degree of suppression is strongest at 15°, consistent with the other phenotypic effects described for the *sel-10 (n1077)* allele (Jager *et al.* 2004). The behavior of *sel-10* mutant alleles in the *aph-1(zu147)* mutant background supports the model that in the embryo, SEL-10 may be involved in Notch downregulation, but that this role may be redundant with other proteins whose participation in Notch downregulation is interrupted by the presence of the SEL-10 (G567E) dominant negative protein.

Given the similar suppressive effects of *sel-10(n1077)* and *sao-1* mutations on *aph-1(zu147)*, we examined whether *sao-1* might be involved in other documented roles of *sel-10*. Mutations in *sel-10* elevate LIN-12 signaling in worms that have mutant *lin-12* receptor or compromised *sel-12* presenilin function (Sundaram and Greenwald 1993; Hubbard *et al.* 1997; Wu *et al.* 1998; Jager *et al.* 2004) but we found no evidence for *sao-1* function in these roles: *sao-1* mutations did not suppress or enhance the Egl defect of *lin-12* or *sel-12* mutations (Table S1 and Table S2) and *sao-1* mutations did not improve uterine π-cell development in *sel-12* mutants or AC specification of *lin-12* mutants (Table S1 and Table S3). SEL-10 also functions outside of the Notch signaling pathway to influence somatic sex determination (Jager *et al.* 2004), but *sao-1* mutations do not cause the masculinization effects described for *sel-10* mutations (Table S4). The fact that *sao-1* mutations do not mimic all *sel-10* mutant phenotypes suggests that the roles of SAO-1 and SEL-10 may overlap in some cases, such as in the downregulation of GLP-1 signaling in the germ line and early embryo, but not in other cases, such as vulval and uterine fate specification, where SEL-10 may function without SAO-1.

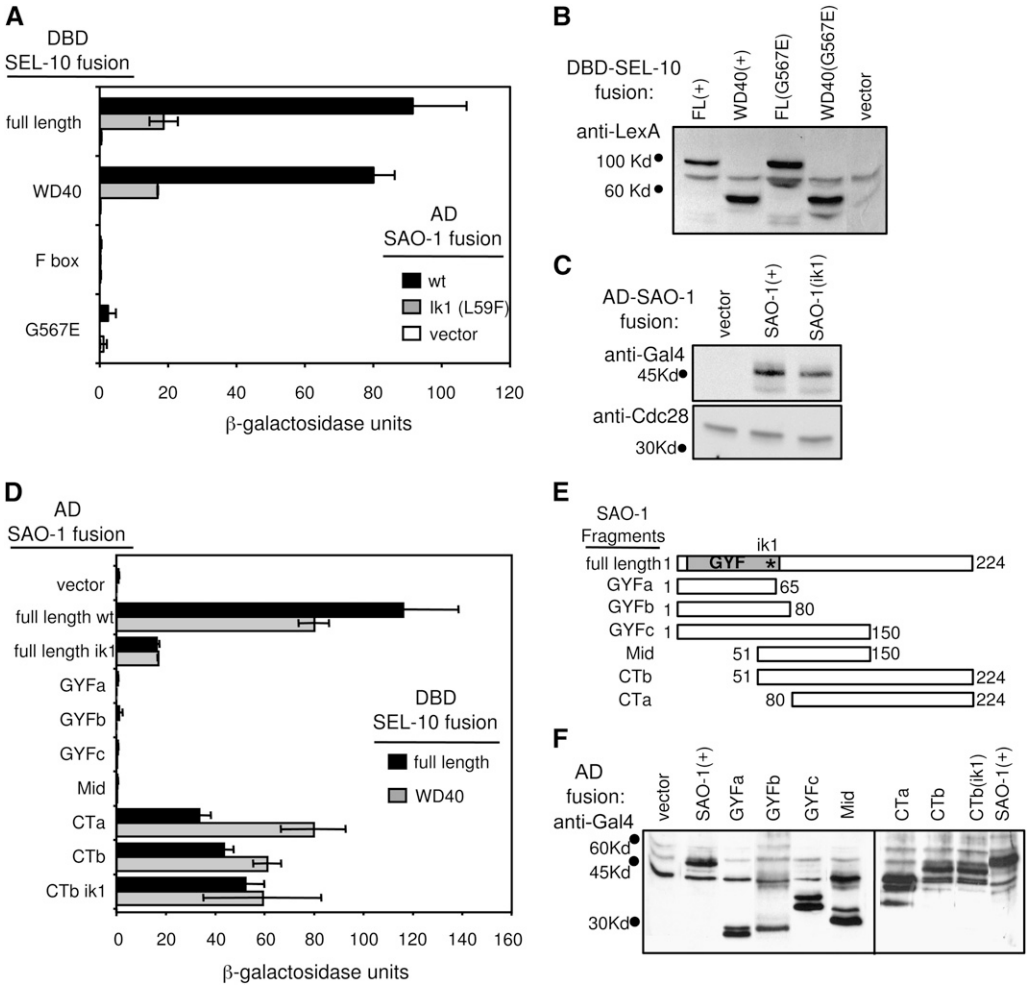

Figure 3 Analysis of SAO-1–SEL-10 protein–protein interaction by yeast two-hybrid analysis. (A) Graph of β-galactosidase units measured for different pairwise combinations of fusion constructs: DNA binding domain (DBD) SEL-10 fusion constructs are indicated on the left and tested against activation domain (AD) alone (vector, white bars) or AD fused to either wild-type SAO-1 (black bars) or SAO-1 (ik1) (gray bars). Residues in SEL-10 fusions are 14–587 (full length and G567E); 178–587 (WD40); 14–179 (F box); G567E is the mutation introduced by *sel-10(n1077)*. (B, C, and F) Detection of fusion proteins expressed in diploid yeast strains used in β-galactosidase experiments. Yeast extracts were probed with antiserum against LexA for DBD fusion detection (B), or against Gal4 for AD fusion detection (C and F), or against Cdc28 as a control for protein levels (C). All strains tested in B also expressed the AD–SAO-1 fusion, and similar results were obtained with strains that did not express an AD fusion. All strains tested in C also expressed the DBD–SEL-10 fusion, and similar results were obtained with strains expressing SEL-10 WD40 DBD or no DBD fusion at all. Positions of molecular weight markers are indicated; the most prominent band detected corresponds to the predicted size for the indicated fusion protein. The AD domain alone is detected as a 15-kDa band, and the DBD domain alone is detected as a 23-kDa band (not shown). FL, full length. (D) Graph of β-galactosidase units measured for different pairwise combinations of fusion constructs: AD fusions with SAO-1 derivatives are indicated on the left and tested against DBD–SEL-10 full-length (solid bars) or DBD–SEL-10 WD40 domain (shaded bars) fusion constructs; "vector" refers to a control construct in which nothing is fused to the AD. β-Galactosidase measurements are reported in standard β-galactosidase units (see *Materials and Methods*); each value is the average of at least three independent experiments. Error bars represent standard deviations (those that are less than two units do not show up on the graph). (E) Schematic representation of the SAO-1 protein and the derivatives that were tested in D. The complete SAO-1 protein is represented on the top row with the GYF domain boxed and the position of the *ik1* missense mutation indicated with an asterisk. Numbers indicate terminal amino acid numbers relative to the intact SAO-1 sequence.

Discussion

To uncover the cellular mechanisms that regulate Notch signaling components in the early *C. elegans* embryo, we used a genetically sensitized system in which one member of the γ-secretase complex, APH-1, was compromised and could mediate only very limited embryonic Notch signaling. We identified *sao-1* as a new gene that negatively impinges on Notch signaling during early embryogenesis and also during larval/adult germline development. Mutations that compromise Notch signaling at the level of receptor (*glp-1*), γ-secretase (*aph-1*), or downstream transcription factor (*lag-1*), all show sensitivity to *sao-1* activity. The *aph-1 (zu147)* embryonic lethality is fully suppressed when SAO-1 function is removed by RNAi or by gene deletion, and even reducing *sao-1* gene dosage by half results in partial suppression. The genetic behavior of *sao-1* mutations suggests that the wild-type gene product antagonizes one or more components of the Notch signaling pathway during embryogenesis and germline development.

A possible mechanism by which SAO-1 may downregulate Notch signaling is suggested by its specific interaction with the Fbw7 protein SEL-10, which functions in substrate recognition for SCF-type E3 ubiquitin ligases. SEL-10 has been shown to directly bind Notch and presenilins and to facilitate their ubiquitination and degradation by the proteasome (reviewed in Lai 2002). The relevance of the SAO-1–SEL-10 interaction to the ability of SAO-1 to antagonize Notch signaling is supported by the observation that missense mutations in SAO-1 or in SEL-10 that disrupt the SAO-1–SEL-10 interaction are also found to cause *aph-1(zu147)* suppression (Figure 3 and Tables 1 and 5).

Table 5 Suppression of aph-1(zu147) by sel-10(n1077)

Genotype of mother	Temperature	% viable progeny (*n*)
aph-1(zu147)	20°	0.7 (1013)
aph-1(zu147); sel-10(ar41)[a]	20°	1.3 (1169)
aph-1(zu147); sel-10(bc243)	20°	0.5 (427)
aph-1(zu147); sel-10(n1077)	20°	6.7 (597)*
aph-1(zu147)	15°	2.1 (448)
aph-1(zu147); sel-10(n1077)	15°	12 (613)*

Embryos were collected from at least 10 mothers of the indicated genotype. All animals were also homozygous for *unc-29(e1072)*. Viable progeny are those that reach at least the L4 stage. *n*, number of embryos scored. A two-tailed Fisher exact test was performed for each value obtained with a *sel-10* mutant relative to the single *aph-1* mutant at the same temperature; an asterisk indicates a difference between the single and double mutant values that is statistically significant with a *P* value <0.0001.

[a] These animals were also homozygous for *lon-3(e2175)*.

Given that the WD40 domain of Fbw7 proteins is responsible for substrate recognition by $SCF^{SEL\text{-}10}$ ubiquitin ligases, the fact that this is the domain of SEL-10 that interacts with SAO-1 is consistent with two alternative models: either SAO-1 is recognized as a substrate of $SCF^{SEL\text{-}10}$-mediated ubiquitination and degradation or SAO-1 acts as a cofactor with $SCF^{SEL\text{-}10}$ to participate in target recognition and/or ubiquitination. The second model is supported by the parallel phenotypic effects of *sao-1* and *sel-10*. First, mutations in either *sel-10* or *sao-1* can elevate Notch signaling in *aph-1 (zu147)* embryos (this work). Second, removing SAO-1 or SEL-10 activity appears to elevate Notch signaling in *glp-1 (ar202)* mutants (this work and Pepper *et al.* 2003). Third, reduced Notch receptor activity can be increased by removing SAO-1 or SEL-10: this is demonstrated by the suppression of *glp-1(lf)* sterility by *sao-1* mutations (this work) and the suppression of *lin-12(lf)* vulval defects by *sel-10* mutations (Sundaram and Greenwald 1993). Although our results are consistent with the ultimate effect of SAO-1 activity being proteasomal degradation of ubiquitinated targets, it remains possible that any role for SAO-1 in $SCF^{SEL\text{-}10}$-mediated ubiquitination may regulate Notch signaling through other mechanisms, such as effects on receptor endocytosis, protein trafficking, or lysosome-mediated degradation (Mukhopadhyay and Riezman 2007; Fortini and Bilder 2009).

Accessory proteins have not yet been discovered for substrate recognition by Fbw7-based SCF complexes; however, examples of such cofactors do exist among other types of ubiquitin ligases. For example, the SCF^{Skp2} complex employs the leucine-rich repeat of Skp2 for substrate recruitment, but also requires the accessory protein Cks1 for recognition of particular substrates (Ganoth *et al.* 2001; Spruck *et al.* 2001), and substrate recognition by the FEM-1 component of the CUL2-based E3 ubiquitin ligase requires two accessory proteins, FEM-2 and FEM-3, that are not part of the core ligase complex (Starostina *et al.* 2007). Our analysis introduces SAO-1 as a possible Fbw7 cofactor; future molecular work will test this idea and the more general notion that Fbw7 proteins might employ cofactors to diversify their substrate selectivity.

While our results suggest that SAO-1 antagonizes Notch pathway activity, its immediate targets are unknown. SEL-10–mediated ubiquitination has been shown to directly target Notch receptors and presenilins to promote their degradation; the accessibility of one or both of these target proteins in the embryo may be affected by SAO-1 activity, and the stabilization of either of these proteins could account for the observed genetic interactions between *sao-1* mutations and *aph-1*, *glp-1*, or *lag-1* mutations. However, at present it is equally plausible that alternative or additional Notch signaling components are targets of SAO-1 and/or SEL-10. An intriguing possibility is the REF-1 family of transcription factors that are expressed upon Notch activation in each of the early embryonic signaling events. Low levels of embryonic Notch signaling could be amplified by stabilizing the REF-1 proteins. Interestingly, REF-1 proteins have been shown to repress the transcription of LIN-12, LAG-2, and the TBX-37 and TBX-38 transcription factors, thereby preventing cells from participating in subsequent Notch signaling events (Neves and Priess 2005). Neves and Priess have speculated that rapid degradation of REF-1 proteins must occur to derepress LIN-12 expression in descendant cells. A role for SAO-1 in REF-1 degradation could explain the embryonic lethality caused by *sao-1* mutations in *glp-1*–deficient embryos: SAO-1 removal would stabilize REF-1 proteins, and thereby prevent normal embryonic *lin-12* expression, creating a situation that would not be detrimental to embryos (because of the redundancy of *lin-12* and *glp-1*) unless the embryo also has reduced *glp-1* function, as in the case of the *glp-1(lf)*; *sao-1* mutants analyzed here.

SAO-1 does not appear to be an obligate partner of SEL-10 because loss of SAO-1 has no impact on several other processes that are affected by SEL-10, such as AC/ventral uterine cell specification, uterine π-cell specification, and somatic sex determination (Tables S1, Table S2, Table S3, and Table S4). In these contexts, the absence of SAO-1 or the inability of SEL-10 to interact with SAO-1 does not prevent SEL-10 from downregulating its targets. The difference between events that require SEL-10 and SAO-1 *vs.* those that require only SEL-10 could have to do with the specific substrate, such as GLP-1 *vs.* LIN-12 or with the specific cellular context, such as germline *vs.* somatic tissue, since we have observed an effect of SAO-1 on GLP-1–mediated germline events, but not on LIN-12–mediated somatic events. If SAO-1 functions as a SEL-10 cofactor, it might act to broaden the repertoire of SEL-10 substrates, such that a distinct array of substrates are recognized by SAO-1–containing tissues compared to tissues that lack SAO-1.

SAO-1 may also be able to influence Notch signaling without SEL-10, via interactions with alternative proteins. This notion is supported by the fact that embryonic Notch signaling can be increased in *aph-1(zu147)* embryos by completely removing *sao-1* activity, but not by completely removing *sel-10* activity, suggesting that SAO-1–mediated downregulation can still occur in the absence of SEL-10. By contrast, the dominant negative SEL-10(G567E) protein, encoded by *sel-10(n1077)*, interferes with Notch downregulation in the embryo. This effect is similar to that of *sel-10* mutations in the context of HSN development, where *sel-10*

(n1077), but not *sel-10(null)*, causes a mutant phenotype and contrasts with the effect of *sel-10* mutations on vulval development, where *sel-10(n1077)* causes the same defective phenotype as caused by *sel-10(null)* (Jager *et al.* 2004). Jager and colleagues proposed that the HSN precursor cells might contain alternative F-box proteins that could substitute for SEL-10 in its absence, but that nonfunctional $SCF^{SEL\text{-}10(G567E)}$ complexes might prevent such substitution, resulting in a more severe phenotype for *sel-10(n1077)* than *sel-10(null)*. Our results are consistent with this model and suggest that the embryo may contain F-box proteins that can act redundantly with SEL-10. Thus SEL-10–deficient embryos may be able to assemble alternative SCF complexes that can interact with SAO-1, providing a different route to SAO-1–mediated downregulation of Notch signaling.

Although we have identified SAO-1 and studied its role in relationship to Notch signaling, several clues suggest that SAO-1 function is not limited to the Notch pathway. First, worms that are deficient in *sao-1* function and raised at 25° exhibit several incompletely penetrant phenotypes, some of which do not resemble known Notch mutant phenotypes (such as high incidence of males and egg retention). Second, in a study of germ line-expressed genes, *sao-1* was classified among the 157 most highly expressed genes (out of a total of 4699 germ line-expressed genes; Wang *et al.* 2009). Other highly expressed genes in this study include genes involved in translation, RNA binding, and ubiquitin/proteasome protein degradation; in contrast Notch signaling components are expressed at much more modest levels. A third hint that *sao-1* may be involved in processes other than Notch signaling comes from its identification as one of 21 RNAi targets that can suppress the cytokinesis defects of *rfl-1* mutant embryos (Dorfman *et al.* 2009). Interestingly, this screen also identified *sel-10*(RNAi) as a modulator of *rfl-1* activity; however, the effect of *sel-10* RNAi was opposite to that of *sao-1* RNAi. The RFL-1 gene product is part of the Nedd8 protein conjugation pathway that neddylates cullin-based E3 ubiquitin ligases and could represent another target of SAO-1–SEL-10 combined activity.

SAO-1 provides a useful model with which to study the roles of GYF-domain proteins in a genetically tractable animal system. GYF-domain–containing proteins generally do not contain additional shared sequence motifs, suggesting that this domain is a self-contained module used in proteins of various functions. The *C. elegans* genome contains three additional genes that encode well-conserved GYF domains, but none show any sequence similarity with SAO-1 outside of the GYF domain (Kofler and Freund 2006). In yeast, GYF-domain proteins have been associated with a variety of cellular functions, such as COPII vesicle formation (Higashio *et al.* 2008), membrane traffic (Georgiev *et al.* 2008), gene-specific inhibition of translation initiation (Sezen *et al.* 2009), and mRNA splicing (Bialkowska and Kurlandzka 2002). Identification of binding partners for human GYF domains also supports involvement in vesicle transport and mRNA processing (Kofler *et al.* 2009; Ash *et al.* 2010). The GYF domain of SAO-1 most closely resembles those of the SMY-2 class of GYF domains, which includes the mammalian GIGYF1 and GIGYF2 proteins. Disruption of the mouse gene GIGYF2 causes a neurodegenerative phenotype as well as altered insulin receptor function (Giovannone *et al.* 2009), but the molecular connection between these phenotypes and GIGYF2 function remains unknown.

In addition to its GYF domain, SAO-1 contains a C-terminal extension that is conserved among nematode species and is conspicuously enriched in proline residues, including a PPG sequence that is a common recognition sequence for GYF domains (Kofler *et al.* 2005). The presence of a GYF recognition motif in other GYF-domain proteins has been hypothesized to facilitate intramolecular interactions (Freund *et al.* 2003). An intramolecular interaction between the GYF and the C-terminal portion of SAO-1 could explain how the SAO-1–SEL-10 interaction is disrupted by the *sao-1(ik1)* mutation in the GYF domain, despite the GYF domain being dispensable for SAO-1–SEL-10 interaction. For example, the *ik1* mutation might enhance the intramolecular binding of SAO-1, thereby reducing the ability to bind other proteins such as SEL-10. Of course, the SAO-1 GYF domain itself may also be involved in heterotypic interactions with as yet unidentified partners.

Although the precise molecular function of SAO-1 remains unknown, our analyses of various physical and genetic interactions support a simple model in which SAO-1 acts as a co-factor along with the SEL-10 substrate-recognition moiety of the SCF ubiquitin ligase to downregulate one or more components of Notch signaling. The effect of preventing this interaction (*e.g.*, by decreasing SAO-1 levels or by disrupting the SAO-1–SEL-10 interaction through point mutations in either protein) appears to be an increase in Notch signaling in certain compromised settings. While the SEL-10 protein and its role in Notch downregulation is structurally and functionally conserved, the SAO-1 protein does not have obvious orthologs in other organisms. This lack of conservation may reflect the diversity of substrates that are recognized by SCF^{Fbw7} complexes and the variety of proteins that may prove to associate with conserved SCF^{Fbw7} complexes to alter their interaction with substrates. While SAO-1 is important during germline and early embryonic development, unrelated but functionally analogous proteins might contribute to Fbw7 substrate specificity in other tissues and stages. Hence, further exploration of the molecular role of SAO-1 will provide a useful model for GYF-domain function, SCF accessory factors, and Notch pathway regulators in a variety of animal systems.

Acknowledgments

We are grateful to Jim Priess in whose laboratory the feasibility of an *aph-1* suppressor screen was first explored. We thank Barbara Conradt, Iva Greenwald, Wendy Hanna-Rose, Oliver Hobert, Jane Hubbard, Judith Kimble, Jim Priess, and Peter Pryciak for strains and reagents. We thank Shin Yi Lin, Josette Manzano, Ellen Leffler, Carolyn Koularis, Elinor Lee, Leigh Harris, Allyson Rinderle, Rebecca Resnick,

and Clare Howard for contributions to this work and anonymous reviewers for thoughtful comments on the manuscript. Some strains used in this work were supplied by the *Caenorhabditis* Genetics Center, which is funded by the National Institutes of Health (NIH) National Center for Research Resources. The *sao-1(ok3335)* allele was generated and provided by the *Caenorhabditis elegans* Gene Knockout Consortium (University of Minnesota), which is funded by the NIH. This research was supported by the National Science Foundation (grant IBN-0131657).

Literature Cited

Ash, M. R., K. Faelber, D. Kosslick, G. I. Albert, Y. Roske *et al.*, 2010 Conserved beta-hairpin recognition by the GYF domains of Smy2 and GIGYF2 in mRNA surveillance and vesicular transport complexes. Structure 18: 944–954.

Berry, L. W., B. Westlund, and T. Schedl, 1997 Germ-line tumor formation caused by activation of glp-1, a Caenorhabditis elegans member of the Notch family of receptors. Development 124: 925–936.

Bialkowska, A., and A. Kurlandzka, 2002 Proteins interacting with Lin 1p, a putative link between chromosome segregation, mRNA splicing and DNA replication in Saccharomyces cerevisiae. Yeast 19: 1323–1333.

Bosu, D. R., and E. T. Kipreos, 2008 Cullin-RING ubiquitin ligases: global regulation and activation cycles. Cell Div. 3: 7.

Brenner, S., 1974 The genetics of Caenorhabditis elegans. Genetics 77: 71–94.

Dalfó, D., J. R. Priess, R. Schnabel and E. J. Hubbard, 2010 glp-1 (e2141) sequence correction, *The Worm Breeder's Gazette*. Avalaible at: http://www.wormbook.org/wbg/archives/volume-18-number-3/.

de Souza, N., L. G. Vallier, H. Fares, and I. Greenwald, 2007 SEL-2, the C. elegans neurobeachin/LRBA homolog, is a negative regulator of lin-12/Notch activity and affects endosomal traffic in polarized epithelial cells. Development 134: 691–702.

Dorfman, M., J. E. Gomes, S. O'Rourke, and B. Bowerman, 2009 Using RNA interference to identify specific modifiers of a temperature-sensitive, embryonic-lethal mutation in the Caenorhabditis elegans ubiquitin-like Nedd8 protein modification pathway E1-activating gene rfl-1. Genetics 182: 1035–1049.

Fortini, M. E., 2009 Notch signaling: the core pathway and its posttranslational regulation. Dev. Cell 16: 633–647.

Fortini, M. E., and D. Bilder, 2009 Endocytic regulation of Notch signaling. Curr. Opin. Genet. Dev. 19: 323–328.

Francis, R., G. McGrath, J. Zhang, D. A. Ruddy, M. Sym *et al.*, 2002 aph-1 and pen-2 are required for Notch pathway signaling, gamma-secretase cleavage of betaAPP, and presenilin protein accumulation. Dev. Cell 3: 85–97.

Freund, C., R. Kuhne, S. Park, K. Thiemke, E. L. Reinherz *et al.*, 2003 Structural investigations of a GYF domain covalently linked to a proline-rich peptide. J. Biomol. NMR 27: 143–149.

Ganoth, D., G. Bornstein, T. K. Ko, B. Larsen, M. Tyers *et al.*, 2001 The cell-cycle regulatory protein Cks1 is required for SCF(Skp2)-mediated ubiquitinylation of p27. Nat. Cell Biol. 3: 321–324.

Georgiev, A., A. Leipus, I. Olsson, J. M. Berrez, and A. Mutvei, 2008 Characterization of MYR1, a dosage suppressor of YPT6 and RIC1 deficient mutants. Curr. Genet. 53: 235–247.

Giovannone, B., W. G. Tsiaras, S. de la Monte, J. Klysik, C. Lautier *et al.*, 2009 GIGYF2 gene disruption in mice results in neurodegeneration and altered insulin-like growth factor signaling. Hum. Mol. Genet. 18: 4629–4639.

Goutte, C., M. Tsunozaki, V. A. Hale, and J. R. Priess, 2002 APH-1 is a multipass membrane protein essential for the Notch signaling pathway in Caenorhabditis elegans embryos. Proc. Natl. Acad. Sci. USA 99: 775–779.

Grant, B., and I. Greenwald, 1996 The Caenorhabditis elegans sel-1 gene, a negative regulator of lin-12 and glp-1, encodes a predicted extracellular protein. Genetics 143: 237–247.

Greenwald, I., 2005 LIN-12/Notch signaling in C. elegans. WormBook: 1–16.

Gupta-Rossi, N., O. Le Bail, H. Gonen, C. Brou, F. Logeat *et al.*, 2001 Functional interaction between SEL-10, an F-box protein, and the nuclear form of activated Notch1 receptor. J. Biol. Chem. 276: 34371–34378.

Hanna-Rose, W., and M. Han, 1999 COG-2, a sox domain protein necessary for establishing a functional vulval-uterine connection in Caenorhabditis elegans. Development 126: 169–179.

Higashio, H., K. Sato, and A. Nakano, 2008 Smy2p participates in COPII vesicle formation through the interaction with Sec23p/Sec24p subcomplex. Traffic 9: 79–93.

Hollenberg, S. M., R. Sternglanz, P. F. Cheng, and H. Weintraub, 1995 Identification of a new family of tissue-specific basic helix-loop-helix proteins with a two-hybrid system. Mol. Cell. Biol. 15: 3813–3822.

Hubbard, E. J., G. Wu, J. Kitajewski, and I. Greenwald, 1997 sel-10, a negative regulator of lin-12 activity in Caenorhabditis elegans, encodes a member of the CDC4 family of proteins. Genes Dev. 11: 3182–3193.

Hutter, H., and R. Schnabel, 1994 glp-1 and inductions establishing embryonic axes in C. elegans. Development 120: 2051–2064.

Jager, S., H. T. Schwartz, H. R. Horvitz, and B. Conradt, 2004 The Caenorhabditis elegans F-box protein SEL-10 promotes female development and may target FEM-1 and FEM-3 for degradation by the proteasome. Proc. Natl. Acad. Sci. USA 101: 12549–12554.

Killian, D. J., E. Harvey, P. Johnson, M. Otori, S. Mitani *et al.*, 2008 SKR-1, a homolog of Skp1 and a member of the SCF (SEL-10) complex, regulates sex-determination and LIN-12/Notch signaling in C. elegans. Dev. Biol. 322: 322–331.

Kim, S. K., J. Lund, M. Kiraly, K. Duke, M. Jiang *et al.*, 2001 A gene expression map for Caenorhabditis elegans. Science 293: 2087–2092.

Kimble, J., and S. L. Crittenden, 2005 Germline proliferation and its control. WormBook: 1–14.

Kodoyianni, V., E. M. Maine, and J. Kimble, 1992 Molecular basis of loss-of-function mutations in the glp-1 gene of Caenorhabditis elegans. Mol. Biol. Cell 3: 1199–1213.

Kofler, M. M., and C. Freund, 2006 The GYF domain. FEBS J. 273: 245–256.

Kofler, M., K. Motzny, and C. Freund, 2005 GYF domain proteomics reveals interaction sites in known and novel target proteins. Mol. Cell. Proteomics 4: 1797–1811.

Kofler, M., M. Schuemann, C. Merz, D. Kosslick, A. Schlundt *et al.*, 2009 Proline-rich sequence recognition: I. Marking GYF and WW domain assembly sites in early spliceosomal complexes. Mol. Cell. Proteomics 8: 2461–2473.

Kopan, R., and M. X. Ilagan, 2009 The canonical Notch signaling pathway: unfolding the activation mechanism. Cell 137: 216–233.

Kushnirov, V. V., 2000 Rapid and reliable protein extraction from yeast. Yeast 16: 857–860.

Lai, E. C., 2002 Protein degradation: four E3s for the notch pathway. Curr. Biol. 12: R74–R78.

Lambie, E. J., and J. Kimble, 1991 Two homologous regulatory genes, lin-12 and glp-1, have overlapping functions. Development 112: 231–240.

Li, J., A. M. Pauley, R. L. Myers, R. Shuang, J. R. Brashler *et al.*, 2002 SEL-10 interacts with presenilin 1, facilitates its ubiquitination, and alters A-beta peptide production. J. Neurochem. 82: 1540–1548.

Li, S., C. M. Armstrong, N. Bertin, H. Ge, S. Milstein *et al.*, 2004 A map of the interactome network of the metazoan C. elegans. Science 303: 540–543.

Mango, S. E., E. M. Maine, and J. Kimble, 1991 Carboxy-terminal truncation activates glp-1 protein to specify vulval fates in Caenorhabditis elegans. Nature 352: 811–815.

Mourikis, P., R. J. Lake, C. B. Firnhaber, and B. S. DeDecker, 2010 Modifiers of notch transcriptional activity identified by genome-wide RNAi. BMC Dev. Biol. 10: 107.

Mukhopadhyay, D., and H. Riezman, 2007 Proteasome-independent functions of ubiquitin in endocytosis and signaling. Science 315: 201–205.

Neves, A., and J. R. Priess, 2005 The REF-1 family of bHLH transcription factors pattern C. elegans embryos through Notch-dependent and Notch-independent pathways. Dev. Cell 8: 867–879.

Parks, A. L., and D. Curtis, 2007 Presenilin diversifies its portfolio. Trends Genet. 23: 140–150.

Pepper, A. S., D. J. Killian, and E. J. Hubbard, 2003 Genetic analysis of Caenorhabditis elegans glp-1 mutants suggests receptor interaction or competition. Genetics 163: 115–132.

Petroski, M. D., and R. J. Deshaies, 2005 Function and regulation of cullin-RING ubiquitin ligases. Nat. Rev. Mol. Cell Biol. 6: 9–20.

Priess, J. R., 2005 Notch signaling in the C. elegans embryo. WormBook: 1–16.

Priess, J. R., H. Schnabel, and R. Schnabel, 1987 The glp-1 locus and cellular interactions in early C. elegans embryos. Cell 51: 601–611.

Pryciak, P. M., and L. H. Hartwell, 1996 AKR1 encodes a candidate effector of the G beta gamma complex in the Saccharomyces cerevisiae pheromone response pathway and contributes to control of both cell shape and signal transduction. Mol. Cell. Biol. 16: 2614–2626.

Qiao, L., J. L. Lissemore, P. Shu, A. Smardon, M. B. Gelber *et al.*, 1995 Enhancers of glp-1, a gene required for cell-signaling in Caenorhabditis elegans, define a set of genes required for germline development. Genetics 141: 551–569.

Reinke, V., H. E. Smith, J. Nance, J. Wang, C. Van Doren *et al.*, 2000 A global profile of germline gene expression in C. elegans. Mol. Cell 6: 605–616.

Sezen, B., M. Seedorf, and E. Schiebel, 2009 The SESA network links duplication of the yeast centrosome with the protein translation machinery. Genes Dev. 23: 1559–1570.

Spieth, J., G. Brooke, S. Kuersten, K. Lea, and T. Blumenthal, 1993 Operons in C. elegans: polycistronic mRNA precursors are processed by trans-splicing of SL2 to downstream coding regions. Cell 73: 521–532.

Spruck, C., H. Strohmaier, M. Watson, A. P. Smith, A. Ryan *et al.*, 2001 A CDK-independent function of mammalian Cks1: targeting of SCF(Skp2) to the CDK inhibitor p27Kip1. Mol. Cell 7: 639–650.

Starostina, N. G., J. M. Lim, M. Schvarzstein, L. Wells, A. M. Spence *et al.*, 2007 A CUL-2 ubiquitin ligase containing three FEM proteins degrades TRA-1 to regulate C. elegans sex determination. Dev. Cell 13: 127–139.

Sundaram, M., and I. Greenwald, 1993 Suppressors of a lin-12 hypomorph define genes that interact with both lin-12 and glp-1 in Caenorhabditis elegans. Genetics 135: 765–783.

Sze, J. Y., M. Victor, C. Loer, Y. Shi, and G. Ruvkun, 2000 Food and metabolic signalling defects in a Caenorhabditis elegans serotonin-synthesis mutant. Nature 403: 560–564.

Verheyen, E. M., K. J. Purcell, M. E. Fortini, and S. Artavanis-Tsakonas, 1996 Analysis of dominant enhancers and suppressors of activated Notch in Drosophila. Genetics 144: 1127–1141.

Walhout, A. J., R. Sordella, X. Lu, J. L. Hartley, G. F. Temple *et al.*, 2000 Protein interaction mapping in C. elegans using proteins involved in vulval development. Science 287: 116–122.

Wang, M., and P. W. Sternberg, 2000 Patterning of the C. elegans 1 degrees vulval lineage by RAS and Wnt pathways. Development 127: 5047–5058.

Wang, X., Y. Zhao, K. Wong, P. Ehlers, Y. Kohara *et al.*, 2009 Identification of genes expressed in the hermaphrodite germ line of C. elegans using SAGE. BMC Genomics 10: 213.

Welcker, M., and B. E. Clurman, 2008 FBW7 ubiquitin ligase: a tumour suppressor at the crossroads of cell division, growth and differentiation. Nat. Rev. Cancer 8: 83–93.

Wen, C., and I. Greenwald, 1999 p24 proteins and quality control of LIN-12 and GLP-1 trafficking in Caenorhabditis elegans. J. Cell Biol. 145: 1165–1175.

Wu, G., E. J. Hubbard, J. K. Kitajewski, and I. Greenwald, 1998 Evidence for functional and physical association between Caenorhabditis elegans SEL-10, a Cdc4p-related protein, and SEL-12 presenilin. Proc. Natl. Acad. Sci. USA 95: 15787–15791.

Wu, G., S. Lyapina, I. Das, J. Li, M. Gurney *et al.*, 2001 SEL-10 is an inhibitor of notch signaling that targets notch for ubiquitin-mediated protein degradation. Mol. Cell. Biol. 21: 7403–7415.

Communicating editor: B. J. Meyer

GENETICS

Supporting Information
http://www.genetics.org/content/suppl/2011/12/30/genetics.111.136804.DC1

Notch Signaling Is Antagonized by SAO-1, a Novel GYF-Domain Protein That Interacts with the E3 Ubiquitin Ligase SEL-10 in *Caenorhabditis elegans*

Valerie A. Hale, Evan L. Guiney, Lindsey Y. Goldberg, Josephine H. Haduong, Callie S. Kwartler, Katherine W. Scangos, and Caroline Goutte

DOI: 10.1534/genetics.111.136804

Table S1 ***sao-1*** **mutations do not affect the Egl defect of** ***lin-12*** **mutations**

Genotype	Temperature	% Egg laying proficiency (n)		
		sao-1(+)	*sao-1(ik1)*	*sao-1(ok3335)*
lin-12(n676n930)[a]	25°	1.6 (121)	2.1 (145)	0 (44)
lin-12(n676n930)[a]	15°	85 (318)	93 (251)	85 (112)
lin-12(n302)[b] */ +*	20°	45 (148)	41 (163)	ND
		% Hermaphrodites with 2AC[d] (n)		
		sao-1(+)	*sao-1(ik1)*	*sao-1(ok3335)*
lin-12(n676n930)[a,c]	25°	30 (94)	30 (113)	36 (33)

Hermaphrodites that were homozygous for either *sao-1(+), sao-1(ik1)* or *sao-1(ok3335)* and also had the indicated *lin-12* genotype were raised at the specified temperature and scored for egg laying proficiency or anchor cell (AC) development. Egg laying proficiency is defined as active laying for at least two consecutive days. n, number of animals scored. ND, not determined.

a *lin-12(n676n930)* causes a loss-of-function phenotype at 25°C and a gain-of-function phenotype at at 15°C(SUNDARAM and GREENWALD 1993a).

b *lin-12(302)* causes a gain-of-function phenotype that is semi-dominant(SUNDARAM and GREENWALD 1993a).

c Strains also contain the integrated AC-specific marker *zmp-1::gfp* which was used to identify ACs in early L4 stage hermaphrodites (pre-vulval indentation) (WANG and STERNBERG 2000).

d For comparison *lin-12(n676n930); sel-10(ar41)* yields only 3% 2AC(SUNDARAM and GREENWALD 1993b).

Table S2 *sao-1* mutations do not suppress the Egl defect of *sel-12*

	% Egg laying proficiency (n)		
Genotype	*sao-1(+)*	*sao-1(ik1)*	*sao-1(ok3335)*
se1-12(ty11)	0 (101)	0 (103)	0 (89)
se1-12(171)[a]	0 (98)	1 (104)	0 (95)
se1-12(131)[a]	0 (96)	4.2 (119)	0 (96)

Hermaphrodites that were homozygous for either *sao-1(+), sao-1(ik1)*, or *sao-1(ok3335)* and also had the indicated *sel-12* genotype were scored for egg laying proficiency. Egg laying proficiency is defined as active laying for at least two consecutive days. n, number of animals scored. ND, not determined.

a For comparison: Egg laying proficiency is observed among 20% of *sel-10(ar41); sel-12(171)* animals and 75% of *sel-10(ar41); sel-12(131)* animals (Wu *et al.* 1998).

Table S3 ***sao-1(ik1)*** **does not improve the uterine π cell defect caused by** ***sel-12(ar171)***

Genotype	Uterine π cells/side (n)
sao-1(+); sel-12(+)	6.05 (38)
sel-12(ar171)[a]	0.11 (56)
sao-1(ik1); sel-12(ar171)[a]	0.09 (56)

The average number of uterine **π** cells per side was determined for mid L4 stage hermaphrodites (Christmas-tree stage) of the indicated genotypes. All strains contained the integrated **π**-cell specific marker *cog-2::gfp(HANNA-ROSE and HAN 1999)*. n, number of animals scored; only one side was counted per animal.
a sel-12(ar171) animals were also homozygous for the marker *unc-1(e538).*

Table S4 ***sao-1(ik1)*** **does not have a masculinizing effect similar to that of** ***sel-10*** **mutations**

Genotype	Temperature	% XX Male development [a] (n)	
		***sao-1*(+)**	***sao-1(ik1)***
tra-2(n1106)	20°	2.5 (321)	2.4 (332)
		% Egl Defect [b] (n)	
		***sao-1*(+)**	***sao-1(ik1)***
sel-10(n1077)/+	15°	28 (141)	28 (136)
sel-10(n1077)/+	20°	22 (106)	17 (135)
		%HSNs present [b] (n)	
		***sao-1*(+)**	***sao-1(ok3335)***
mgIs42 [tph-1::gfp]	20°	90 (55)	93 (80)

Hermaphrodites that were homozygous for either *sao-1(+), sao-1(ik1), or sao-1(ok3335)* and also had the indicated *tra-2*, *sel-10, or mgIs42* genotype were scored for male-type development as follows: *tra-2* animals were scored for development as males based on the presence of a male tail. *sel-10(n1077)/+* animals were scored for the inability to lay eggs (Egl) as an indicator of male-specific development of the hermaphrodite-specific vulval neurons (HSN) (JAGER *et al.* 2004). *mgIs42* animals were scored for the presence of HSN's by virtue of HSN-specific *tph-1::gfp* expression(SZE *et al.* 2000); the reported percentage reflects the number of observed HSN's divided by the total expected number of HSNs, which is twice the number of observed animals since two HSNs are expected in each hermaphrodite. n, number of animals scored.

a For comparison, Jager et al report 25% male-like development among *tra-2(n1106); sel-10(bc243)* animals(JAGER *et al.* 2004), and Desai and Horvitz report that all *tra-2(n1106); sel-10(n1077)* animals are all either male-like or intersexual(DESAI and HORVITZ 1989).

b Homozygous *sel-10(n1077)* hermaphrodites are partially masculinized in that the HSNs fail to develop, causing a fully penetrant Egl defect and observation of only 8% of the expected HSNs(JAGER *et al.* 2004).